A molecular beam study of the H+N3 reaction. Product NH internal state distribution and electronic state branching ratio

Jing Chen, Edwin Quiñones, and Paul J. Dagdigian

Citation: The Journal of Chemical Physics **93**, 4033 (1990); doi: 10.1063/1.458735
View online: http://dx.doi.org/10.1063/1.458735
View Table of Contents: http://scitation.aip.org/content/aip/journal/jcp/93/6?ver=pdfcov
Published by the AIP Publishing

A molecular beam study of the $H+N_3$ reaction. Product NH internal state distribution and electronic state branching ratio

Jing Chen, Edwin Quiñones, and Paul J. Dagdigian
Department of Chemistry, The Johns Hopkins University, Baltimore, Maryland 21218

(Received 7 December 1989; accepted 31 May 1990)

The $H + N_3 \rightarrow NH(X\,^3\Sigma^-, a\,^1\Delta, b\,^1\Sigma^+) + N_2$ reaction has been studied in a molecular beam-gas scattering arrangement in order to determine the nascent product state distribution. The NH product in specific rovibronic/fine-structure states has been detected by laser fluorescence excitation. The relative cross sections for formation of various vibrational levels in the $a\,^1\Delta$ electronic state were determined to equal $1{:}1.0 \pm 0.3{:}1.4 \pm 0.3{:}\leqslant 1.5$ for $v = 0$ through 3, inclusive, while the $v = 0$ to $v = 1$ population ratio in the $X\,^3\Sigma^-$ state was found to be $1{:}0.015 \pm 0.003$. The rotational distributions in all vibronic levels were found to be characterized by temperatures near 300 K, suggestive of relaxation of the nascent rotational distributions. By comparison of the populations of a specific pair of $X\,^3\Sigma^-$ and $a\,^1\Delta$ state levels and with summation over the derived rovibrational distributions, an electronic state branching ratio of 3.2 ± 1.3 was obtained for the $X\,^3\Sigma^-$ to $a\,^1\Delta$ electronic state branching ratio. An upper limit of $\leqslant 0.02$ was also derived for the ratio of the $b\,^1\Sigma^+$ $v = 0$ to $a\,^1\Delta$ $v = 0$ populations. These results are compared with NH fragment distributions observed in the photodissociation of $HN_3(\tilde{X}\,^1A')$ and with our expectations based on our fragmentary knowledge of HN_3 potential energy surfaces.

I. INTRODUCTION

The reaction of an atom with a free radical is an interesting class of chemical reactions whose dynamics has not been extensively studied. A major difficulty with the study of these reactions is that special techniques are required for the preparation of *both* reagents. Thermal rate constants have been measured for a number of atom-radical reactions,[1] and there have been measurements of the product internal state distributions for several such reactions, e.g., $H + NO_2$,[2,3] ClO,[4] SF,[4] and NF_2.[5] Study of the first cited reaction was greatly facilitated by the fact the NO_2 is a stable free radical. Since both reagents in an atom-radical reaction are open-shell species, these reactions necessarily involve multiple potential energy surfaces, and the reaction dynamics can be strongly influenced by couplings between surfaces. In addition, atom-radical reactions will often have access to a strongly bound intermediate, namely the stable molecule which can be formed by the chemical bonding of the reagents.

A particularly interesting class of atom-radical reactions are the reactions of the azide radical N_3. Since the N–N_2 binding energy is quite small, these reactions are highly exothermic. Chemiluminescence spectra and thermal rate constants have been reported for the reaction of N_3 with halogen,[6–9] nitrogen,[6,11–13] oxygen,[6,10,13] phosphorus,[14] arsenic,[15] and carbon[16] atoms. The branching ratio for the production of excited state products has been found to be large for reactions in which the electronic state branching ratio was measured. From measurement of the NF $a\,^1\Delta \rightarrow X\,^3\Sigma^-$ absolute emission intensity, the fraction of NF product from the $F + N_3$ reaction formed in the $a\,^1\Delta$ state was deduced to be greater than ca. 90%.[9] A similar high branching ratio for formation of $NO(A\,^2\Sigma^+)$ was estimated for $O + N_3$.[10,13]

The large yield of electronically excited products in the $X + N_3$ reactions, where X is a halogen atom, can be explained by spin conservation rules. Reaction along a singlet XN_3 surface can proceed without a barrier to the stable $XN_3(\tilde{X}\,^1A')$ intermediate, which decomposes to yield NX in the electronically excited $a\,^1\Delta$ state. By contrast, formation of NX in the ground $X\,^3\Sigma^-$ state requires either a singlet–triplet mixing in the exit channel or direct reaction along a triplet surface, which is likely to have a barrier. Electronic orbital angular momentum conservation arguments have been also presented to explain the high excited state branching ratio in other atom–azide reactions, e.g., $N + N_3$.[12]

In this paper, we present a study of the dynamics of the $H + N_3$ reaction:[17]

$$H(^2S) + N_3(\tilde{X}\,^2\Pi_g) \rightarrow NH + N_2(X\,^1\Sigma_g^+),$$
$$\Delta H_0^0 = -328 \pm 21 \text{ kJ/mole}. \qquad (1)$$

A preliminary report of this experiment has already appeared in print.[18] The reaction exothermicity is sufficient to allow production of NH in its $X\,^3\Sigma^-$, $a\,^1\Delta$, and $b\,^1\Sigma^+$ electronic states. In this study, a beam of hydrogen atoms crosses, in a beam-gas scattering arrangement, the effluent from a discharge-flow prereactor in which the azide radical is prepared. Product NH in specific product rovibronic/fine-structure states is detected by laser fluorescence excitation. The pressure in the scattering chamber is reduced in order to approach single-collision conditions and hence to allow the determination of the nascent NH internal state distribution.

The dynamics of reaction (1) is expected to be similar to that for the $X + N_3$ reactions, except for differences in the reaction exothermicities and the fact that the binding energy of the HN_3 intermediate is larger than for XN_3. The principal advantage of studying reaction (1) is that NH in all energetically accessible electronic states can be sensitively detected by laser fluorescence excitation. Direct detection of NX in its ground electronic state is difficult using the known bound–bound transitions ($a\,^1\Delta \leftarrow X\,^3\Sigma^-$ and $b\,^1\Sigma^+$

$\leftarrow X\,^3\Sigma^-$) since the oscillator strengths for these band systems are very small.[19] However, recently NF($X\,^3\Sigma^-$) produced in the photolysis of NF_2 was detected by laser fluorescence excitation in the b–X band system.[20]

A schematic diagram of the HN_3 potential energy surfaces relevant to the dynamics of reaction (1) is presented in Fig. 1. As can be seen from Fig. 1 and on the basis of the arguments given above for $X + N_3$, we might expect preferential formation of NH($a\,^1\Delta$) through the strongly bound $HN_3(\tilde{X}\,^1A')$ ground state potential energy surface. The ultraviolet photodissociation of electronically excited HN_3 has also been studied by several groups.[21–25] For wavelengths of 248 nm and longer, the NH fragment is observed only in the $a\,^1\Delta$ electronic state. Very recently, the N_2 fragment has been directly detected by resonant-enhanced multiphoton ionization (REMPI) detection and its rotational state distribution determined.[26]

In principle, there are two mechanisms for the formation of ground state NH($X\,^3\Sigma^-$). As in the analogous $X + N_3$ reactions, this species can be produced either by spin–orbit coupling of the HN_3 $\tilde{X}\,^1A'$ and $^3A''$ surfaces near the crossing in the exit channel, or by direct reaction from the reagents along the $^3A''$ surface. The latter would be possible only if there were no barrier on the surface higher than the reagent translational energy. It may be possible to distinguish these two mechanisms from the experimentally observed NH($X\,^3\Sigma^-$) spin–state distribution. In the IRMPD and NH overtone excitation experiments on $HN_3(\tilde{X}\,^1A')$ by King, Stephenson, and coworkers,[27] a significant yield of spin-forbidden NH($X\,^3\Sigma^-$) product, as well as spin-allowed NH($a\,^1\Delta$), is found. They also observed a nonstatistical $X\,^3\Sigma^-$ spin-state distribution, in which only the F_1 and F_3 components had appreciable population. This anomalous distribution was explained by Alexander *et al.*[28] as arising from symmetry restrictions in the singlet–triplet coupling in a planar intermediate. If spin–orbit mixing through a planar complex were the mechanism for formation of NH($X\,^3\Sigma^-$) product in reaction (1), then we might also expect a similar nonstatistical distribution, provided planarity were maintained in the HN_3 intermediate. By contrast, direct formation of NH($X\,^3\Sigma^-$) on the $^3A''$ surface would be expected to yield a statistical spin-state distribution. We might also expect to have a higher $X\,^3\Sigma^-$ to $a\,^1\Delta$ electronic state branching ratio than that observed in the decomposition of $HN_3(\tilde{X}\,^1A')$ if reaction could occur directly on the $^3A''$ surface.

II. EXPERIMENT

The present study was carried out in a molecular beam apparatus, which is schematically illustrated in Fig. 2. A continuous beam of hydrogen atoms was generated in a quartz tube mounted in an extended Evenson-Broida 2450 MHz microwave discharge cavity.[29] Hydrogen atoms flowed through the tube at a pressure of 3 Torr, and traces of water were added to improve the dissociation efficiency. The quartz tube was treated with 1:1 HF/water to minimize atom recombination on the walls.[30] The discharged gas passed through a 0.07 cm orifice at the end of the quartz tube into the source vacuum chamber, which was evacuated with a 6 in. water-baffled diffusion pump. The resulting beam was collimated with a 0.2 cm diam skimmer and entered the scattering chamber. This chamber was evacuated by two 4 in. diffusion pumps. The pressure rise in the scattering chamber was approximately 2×10^{-5} Torr (uncorrected ionization gauge reading) when the H atom beam was turned on.

The azide radical was prepared in a discharge-flow reactor mated to the scattering chamber by the reaction of fluorine atoms with hydrazoic acid:

$$F + HN_3 \rightarrow N_3 + HF, \qquad (2)$$

for which the reaction rate constant k equals 1.1×10^{10} molecule^{-1} cm^3 s^{-1} (Ref. 9). Fluorine atoms were generated by passing CF_4 in a 0.9 cm diam alumina tube through a 2450 MHz microwave discharge. The effluent then flowed through a 20 cm long Pyrex tube coated with fluorine resistant wax (Halocarbon Co.) and then into the scattering

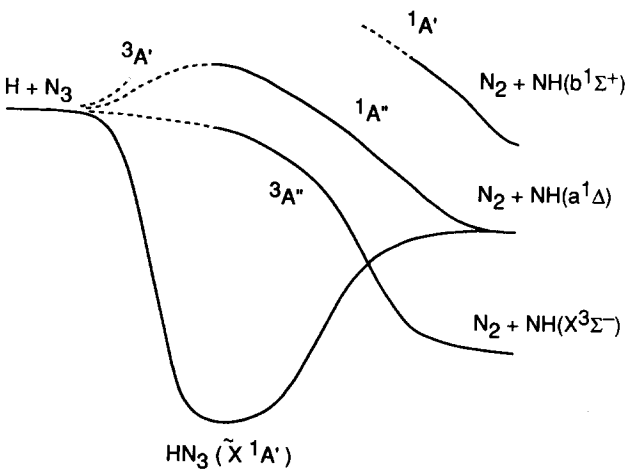

FIG. 1. Schematic reaction coordinate diagram for the low-lying potential energy surfaces relevant to the $H + N_3 \rightarrow NH + N_2$ reaction. The left-hand side represents the approach of the reactants, while the right-hand represents dissociation of the transient HN_3 complex.

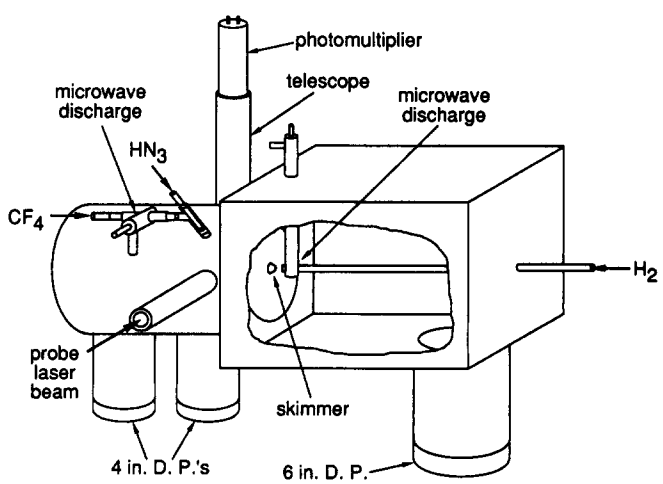

FIG. 2. Diagram of the molecular beam apparatus employed for the study of the $H + N_3$ reaction.

chamber through a 0.2 cm diam Teflon orifice at the end of the tube. The flows in the reactor were so adjusted that at a pressure of 5×10^{-5} Torr in the scattering chamber we could still observe NH products with good signal-to-noise ratio.

Hydrazoic acid was injected into the flow reactor downstream of the microwave discharge with a movable Teflon tube; this allowed adjustment of the length of the F/HN_3 mixing region. The typical mixing time in most experiments was approximately 1 ms. The CF_4 and HN_3 flows were ca. 0.1–0.3 μmole s^{-1}, and the pressure in the reactor was 0.4–0.7 Torr. Other fluorine sources (F_2 and SF_6) were also tried, but the best NH product signals were obtained with CF_4. In our earliest experiments, the azide radical was prepared by thermal decomposition of lead azide at 473 K.[10,13] We verified formation of N_3 by this technique through observation of NO* chemiluminescence from the O + N_3 reaction and detected NH($a\,^1\Delta$) product from reaction (1). We abandoned this generation technique in favor of reaction (2) since the former produced a low concentration of N_3 and the yield was steady for only a short time (1 h).

One of the difficulties in generating N_3 is the ease with which N_3 is destroyed, for example, by further reaction with F atoms [$F + N_3 \rightarrow NF(a\,^1\Delta) + N_2$, $k = 5\times10^{-11}$ molecule^{-1} cm^3 s^{-1}, from Ref. 9] and by self-destruction [$2N_3 \rightarrow 3N_2$, $k = 2\times10^{-11}$ molecule^{-1} cm^3 s^{-1}, from Ref. 9], as well as by wall collisions [estimated as 160 s^{-1} in our reactor by scaling the wall destruction rate of David and Coombe[12(b)] to the diameter of our reactor]. The reactor operation was optimized by monitoring the NH product signal as a function of the flow conditions. For a fixed F atom production, the NH signal would first rise as the HN_3 flow was turned on and then reach a broad maximum, as expected from a kinetic modelling of the concentrations in the reactor. We used nearly equal HN_3 and F concentrations and adjusted the mixing time so that the N_3 density would reach its maximum at the end of the reactor. In early experiments, when the reactor was working much less well, we did observe an artifact NH signal when the F atom microwave discharge was extinguished or the CF_4 flow turned off. Our kinetic modelling indicated that in these runs the HN_3 density in the scattering chamber was about two orders of magnitude higher than that of N_3. A plausible explanation of this false signal is a two-step reaction in the scattering chamber: $H + HN_3 \rightarrow N_3 + H_2$, followed by $H + N_3 \rightarrow NH + N_2$. In our final experiments, this artifact was completely eliminated. When the HN_3 flow was stopped, about 2% of the NH signal remained. We believe that this small signal was due to the reaction of F atoms with HN_3 adsorbed to the walls of the scattering chamber.

The NH products from reaction (1) were detected by laser fluorescence excitation using the frequency-doubled radiation from a XeCl excimer laser pumped dye laser (Lambda Physik EMG101MSC and FL3002E). The spectral linewidth of the laser was typically 0.2 cm^{-1}, but this could be narrowed by insertion of an etalon into the oscillator. The laser beam was directed into the scattering chamber through a set of baffle arms and passed just below the output orifice of the F/HN_3 reactor and 7 cm beyond the H atom skimmer. The diameter of the laser beam in the scattering chamber was 0.6 cm. The fluorescence signal was collected with a three-lens telescope and imaged onto the face of a photomultiplier (EMI 9816B). The output of the latter was amplified by a SR420 preamplifier and fed into a boxcar integrator (SR250). The gate of the boxcar was 500 ns wide and was opened 100 ns after the laser pulse to discriminate against laser scattered light. The laser power was monitored beyond the scattering apparatus with a pyroelectric detector (Molectron J3-0DW), whose output was recorded with a second boxcar integrator. Filters were used to keep this detector in the linear regime when the laser beam was strong. The outputs of the boxcar integrators were acquired and stored on a laboratory computer (Apple Macintosh II) for later analysis.

HN_3 was synthesized from the stearic acid and sodium azide reaction, heated to 400 K.[31] We synthesized up to 150 Torr of HN_3, and no buffer gas was added. The samples were collected in a 5 liter glass bulb covered with wire mesh and inside a box for security. The purity of HN_3 was checked with IR absorption spectroscopy. The main impurities were CO_2 (5%) and H_2O (< 1%). Hydrogen and CF_4 were used directly from the tanks, without further purification.

III. RESULTS

A. Fluorescence excitation spectra

The exothermicity of reaction (1) is sufficient to allow population of the three lowest electronic states of the NH product: $X\,^3\Sigma^-$ (with internal energy up to 92% of the dissociation energy), $a\,^1\Delta$ (in vibrational levels $v\leqslant5$), and $b\,^1\Sigma^+$ ($v\leqslant1$). The energy of the reagents adds slightly more energy. The average reagent collision energy is calculated to be 4 kJ/mole, and the average internal energy of N_3 at 298 K is 4.1 kJ/mole. All these electronic states of NH are conveniently detected in a quantum-state selective manner by laser fluorescence excitation. The particular bands used for excitation and detection are listed in Table I. Because of predissociation in the excited $A\,^3\Pi$ and $c\,^1\Pi$ states,[38,39] the sensi-

TABLE I. Bands used for detection of the various vibronic levels of the NH product.

Vibronic level		Excitation band	Detection band
$X\,^3\Sigma^-$	$v=0$	$A\,^3\Pi - X\,^3\Sigma^-$ (0,0)[a]	$A\,^3\Pi - X\,^3\Sigma^-$ (0,0)
	$v=1$	$A\,^3\Pi - X\,^3\Sigma^-$ (1,1)[a]	$A\,^3\Pi - X\,^3\Sigma^-$ (1,1)
$a\,^1\Delta$	$v=0$	$c\,^1\Pi - a\,^1\Delta$(0,0)[b]	$c\,^1\Pi - a\,^1\Delta$(0,0)
	$v=1$	$c\,^1\Pi - a\,^1\Delta$(0,1)[b]	$c\,^1\Pi - a\,^1\Delta$(0,0)
	$v=2$	$c\,^1\Pi - a\,^1\Delta$(0,2)[c]	$c\,^1\Pi - a\,^1\Delta$(0,0)
	$v=3$	$c\,^1\Pi - a\,^1\Delta$(1,3)[c]	$c\,^1\Pi - a\,^1\Delta$(1,1)
$b\,^1\Sigma^+$	$v=0$	$c\,^1\Pi - b\,^1\Sigma^+$ (0,0)[d]	$c\,^1\Pi - a\,^1\Delta$(0,0)[e]

[a] Reference 32.
[b] Reference 33.
[c] Reference 25.
[d] References 34 and 35.
[e] Radiative decay of the $c\,^1\Pi$ state occurs primarily through transitions to $a\,^1\Delta$, rather than to $b\,^1\Sigma^+$ (Refs. 36 and 37).

tivity for laser fluorescence detection drops rapidly with increasing v.

Figures 3 and 4 presents fluorescence excitation spectra for the $c\,^1\Pi - a\,^1\Delta(0,0)$ and $A\,^3\Pi - X\,^3\Sigma^-$ (0,0) bands, respectively. A spectrum of the c–$a(0,1)$ band was previously reported in our earlier Communication.[18] The c–a band system possesses a relatively simple rotational structure, consisting of P, Q, and R branches. Because of the Λ doubling in both the lower and upper electronic states, all lines are in fact doublets; this splitting becomes progressively larger with increasing J.[33] The Λ doubling was resolved in our spectra at high J (>6) without a line-narrowing etalon in our dye laser (see Fig. 1 of Ref. 18). Use of the etalon allowed resolution of this splitting at low J. The A–X band system has a considerably more complicated rotational structure. In general, $a\,^3\Pi - ^3\Sigma$ band system has 27 allowed rotational branches; however, because the $A\,^3\Pi$ state approaches Hund's case (b) coupling at relatively low J,[32] only 9 of these branches (those for which $\Delta J = \Delta N$) have appreciable intensity for $N \geqslant 7$. Because of the relatively low N levels of NH($X\,^3\Sigma^-$) observed here, a number of "satellite" lines are observed in Fig. 4.

The dependence of the fluorescence signal on laser fluence was measured for the A–$X(0,0)$ band. It was found that the signal was linear with laser pulse energy only at very low laser powers, ca. $\leqslant 0.3$ μJ. This saturation limit was scaled by the known transition probabilities to estimate upper limits for other vibronic bands. When the ratios of certain vibronic bands were measured, the laser energy was kept in the linear regime.

B. Rotational and fine-structure populations in the $X\,^3\Sigma^-$ and $a\,^1\Delta$ states

For the observed fluorescence excitation spectra such as those shown in Figs. 3 and 4, relative rotational populations,

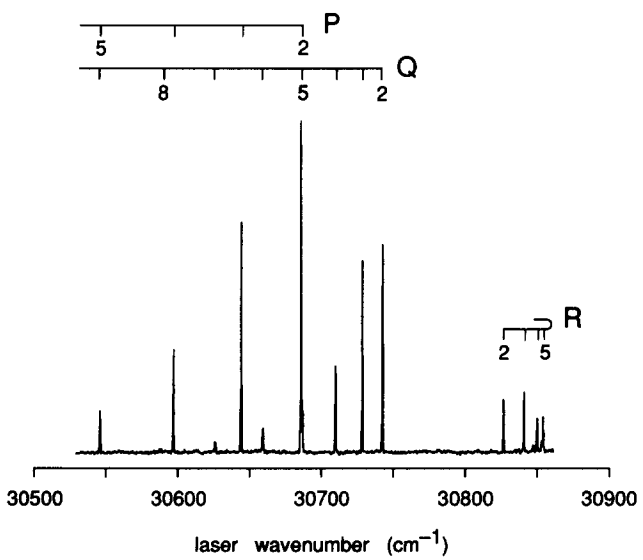

FIG. 3. Laser fluorescence excitation spectrum of the NH $c\,^1\Pi \leftarrow a\,^1\Delta(0,0)$ band from the H + N_3 reaction at 6×10^{-5} Torr pressure in the scattering chamber. Individual rotational lines for detection of the various J levels in the P,Q, and R branches are denoted.

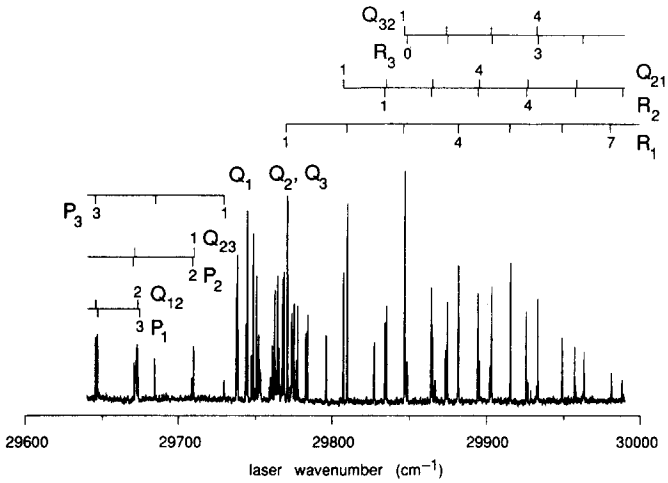

FIG. 4. Laser fluorescence excitation spectrum of the NH $A\,^3\Pi \leftarrow X\,^3\Sigma^-$ (0,0) band from the H + N_3 reaction at 2×10^{-4} Torr pressure in the scattering chamber. Individual rotational lines for detection of the various JF_i levels in various branches are denoted.

as well as the distributions in the $X\,^3\Sigma^-$ spin states and the $a\,^1\Delta$ Λ doublets, were deduced. The relative intensities of the resolved fluorescence lines were converted to populations by means of fluorescence excitation line strength factors calculated using the general formula [Eq. (A1) in the Appendix] given by Greene and Zare[40] for excitation of an isotropic M_J distribution. The calculation of the rotational line strength factors,[41,42] needed in this formula, has been described in detail previously for the $A\,^3\Pi - X\,^3\Sigma^-$ band system.[43] The corresponding factors for the $c\,^1\Pi - a\,^1\Delta$ system may be obtained using the general formulas for a transition between two electronic states both following Hund's case (a) coupling.[41,44] The bandpass filters used in detecting the fluorescence introduced an uneven transmittance of the fluorescence on the various rotational emission lines; this effect was taken into account in converting fluorescence intensities to populations.

For all bands except the very weak A–$X(1,1)$ band, lines of $J \leqslant 9$ were positively identified in the fluorescence excitation spectra. For the $X\,^3\Sigma^-$ $v=0$ and 1 levels, the intensities (peak heights of resolved lines) in the main branches of the A–X (0,0) and (1,1) band could be fit by a Boltzmann distribution in the rotational levels with a "temperature" of 270 ± 20 K and 260 ± 50 K, respectively. For each value of the nuclear rotational angular momentum N, the three spin levels ($\mathbf{J} = \mathbf{N} + \mathbf{S}$) were found to be populated according to their $(2J+1)$ degeneracies.

In determining the rotational populations in the $a\,^1\Delta$ state from the c–a bands, the areas of the lines were used to compute the intensities since the Λ-doublet splitting increases with J and becomes larger than the laser linewidth. Some levels of the excited $c\,^1\Pi$ state are known to predissociate, particularly for $v>0$, and hence have a fluorescence quantum yield Φ of less than unity. The early radiative lifetime measurements by Smith *et al.*[38] showed decreasing values of the radiative lifetime with increasing J for all rotational levels in the $v=0$ vibrational manifold, suggestive of predissociation in all rotational levels. More recent experi-

ments[39] do not show such systematic trend for $J \leqslant 9$. Hence, we shall assume that Φ is unity for all $c\ ^1\Pi\ v=0$ rotational levels excited. The rotational populations of all three observed vibrational levels of the $a\ ^1\Delta$ state can be fit to a Boltzmann form. The derived rotational "temperatures" were found to equal 310 ± 40, 290 ± 40, and 240 ± 60 K for the $a\ ^1\Delta\ v=0$, 1, and 2 vibrational levels, respectively. (The present results correct an erroneous temperature of 750 K for $v=1$ reported in our preliminary Communication.[18]) We also took some careful scans over individual rotational lines in order to measure the relative intensities of the individual Λ doublets. An example of such a scan was shown in the inset of Fig. 1 in our preliminary Communication.[18] We find that the integrated intensities of these doublets were equal to within experimental error ($\pm 2\%$) for all lines examined. The Λ doublet levels are found to be equally populated in all three observed vibrational levels of the NH($a\ ^1\Delta$) product.

One concern in this type of beam-gas scattering arrangement to measure nascent product internal state distributions is the possibility of collisional relaxation by secondary collisions both with other gas molecules and the chamber walls. The observation of near room temperature for the rotational state distribution of the NH($X\ ^3\Sigma^-$) products is suggestive of relaxation of the nascent distribution. We believe that this relaxation is mostly due to collisions with the walls, rather than through gas-phase collisions, since the mean free path for the latter is much greater (ca. 120 cm) than the dimensions of the scattering chamber; in this calculation, we have taken a cross section of 20 Å^2 and a pressure of 0.1 mTorr. In our earlier studies of alkaline earth atom reactions,[45] relaxation by the walls was not a problem since the refractory products would stick to the walls and not be reflected.

Assuming that NH does survive upon collisions with the wall, we can estimate the number of such collisions from the calculated residence time in the scattering chamber, which is given by the ratio of the chamber volume (33 liters) to the pumping speed of the system. The pumping speeds of the two diffusion pumps (taking account of the conductance of the chamber sidearms) are 630 and 300 $l\,s^{-1}$. Thus, the minimum residence time is calculated to equal 35 ms. In this period of time, a molecule would be expected to experience perhaps 76 wall collisions if we take a velocity of 6.5×10^4 cm s^{-1} (average velocity for NH at 300 K) and 17 gas-phase collisions. NH($X\ ^3\Sigma^-$) molecules are relatively unreactive in gas-phase collisions and would be expected to survive upon collisions with the wall. Indeed, long lifetimes for NH(X) have been observed in cell experiments.[46] Thus, the observation of a room-temperature rotational distribution in HN(X) can be explained by equilibrium with the walls.

There is no reliable information on whether NH($a\ ^1\Delta$) can survive wall collisions. The rotational temperature of NH($a\ ^1\Delta$) was found to be approximately room temperature in all detected vibrational levels, independent of the residence time. The latter was increased beyond the minimum value by valving off each of the scattering chamber diffusion pumps in turn. If NH(a) were quenched upon collision with walls, then the rotational temperatures would be representative of the nascent distribution. Alternatively, if NH(a) survives wall collisions, then the nascent distribution could be hotter than that measured here. In Sec. III D, in connection with the measurement of NH product electronic state branching ratio, we attempt to address the question of the wall quenching of NH(a).

C. Vibrational state populations

The relative vibrational populations within each electronic state of the NH product were obtained by comparing the fluorescence intensities of specific rotational lines in different bands and then taking account of the slightly different rotational distribution in each vibronic level. For the $a\ ^1\Delta$ state, this involved comparison of the intensities of the $Q(2)$ lines in the c–a(0,0), (0,1), and (0,2) bands and normalization for the differing laser pulse energies. For the former, frequency doubled radiation was employed, while the latter two bands could be excited with fundamental dye laser outputs. In our analysis, we took account of the fact that the polarization of the doubled radiation was perpendicular to that of the latter. Since the same rotational level in the $c\ ^1\Pi$ state was excited, no correction for differing detection sensitivity was required. These intensity comparisons required changing the laser dye to excite two different bands in the same run; this was facilitated by having two dye circulation modules so that the change could be made quickly.

The relative $a\ ^1\Delta$ vibrational populations are given in Table II. No laser fluorescence signal in the c–a (1,3) band was detected. In estimating an upper bound for the $a\ ^1\Delta\ v=3$ population from the observed noise level, we took account of the fact that the $c\ ^1\Pi\ v=1$ manifold experiences significant predissociation in all rotational levels.[38,39] We also employed the relative spontaneous emission probabilities in the various c–a (1,v) bands recently determined by Nelson and McDonald[25] and assumed that the purely radiative decay rate for $c\ ^1\Pi\ v=1$ was the same as that for $v=0$. The large upper bound on the $v=3$ population reflects the poor Franch–Condon factor for the (1,3) band and the poor detection efficiency due to predissociation in the excited state.

We also investigated the effect of collisional relaxation on the relative vibrational populations in the manner as described in Sec. III B. We found that the $a\ ^1\Delta$ vibrational state distribution was unchanged as the residence time in the scat-

TABLE II. Relative cross sections for formation of various vibronic levels in the NH product of the $H + N_3 \rightarrow NH + N_2$ reaction.[a]

Electronic state	Vibrational level	Cross section
$X\ ^3\Sigma^-$	$v=0$	15.1 ± 4.3
	$v=1$	0.23 ± 0.05
$a\ ^1\Delta$	$v=0$	1[a]
	$v=1$	1.0 ± 0.3
	$v=2$	1.4 ± 0.3
	$v=3$	$\leqslant 1.5$
$b\ ^1\Sigma^+$	$v=0$	$\leqslant 0.02$

[a] Cross sections normalized relative to the $a\ ^1\Delta\ v=0$ manifold.

tering chamber was varied from the minimum attainable time (35 ms) to an order of magnitude greater. If NH($a\ ^1\Delta$) molecules were efficiently quenched upon collisions with the chamber walls, then the $a\ ^1\Delta$ vibrational state distribution would be unaffected by the residence time, and the observed distribution could be equated with the nascent distribution. Alternatively, the observed excited $a\ ^1\Delta$ vibrational population ratios could be equated with the nascent distribution if NH($a\ ^1\Delta$) molecules were inefficiently vibrationally relaxed at the walls, regardless of the efficiency of electronic quenching. As we discuss further in the next section, the latter appears to be the case here.

Comparison of the populations on $v = 0$, 1 levels in the $X\ ^3\Sigma^-$ state is facilitated by the fact that the Q branches of the A–X (1,1) band overlaps the P branches of the (0,0) band of the same electronic transition. The ratio of $v = 1$ vs. $v = 0$ level in the $X\ ^3\Sigma^-$ state is found to be 0.015 ± 0.003. We could observe no dependence of this population ratio on the residence time although the $v = 1$ signal was quite small and hard to measure accurately.

D. Electronic state branching ratios

It is also of great interest to determine the relative populations in the various electronic states of the NH product. The Appendix outlines in detail the determination of these state branching ratios from experimentally measured laser fluorescence intensities in different band systems. This treatment is presented explicitly here since it has not appeared in print previously, and it is possible to ignore unwittingly important factors in this computation.

The ratio of the $X\ ^3\Sigma^-$ to $a\ ^1\Delta$ electronic state populations was obtained from experiments in which the intensities of the R_1 (4) line of A–X (0,0) and $Q(2)$ lines of c–a (0,0) bands were compared under the same flow conditions and detection system settings. These relative intensities were measured using the same dye solution in the dye laser. We found that the ratio of the populations in the detected levels, namely $J = 4\ F_1$ of the $X\ ^3\Sigma^-$ $v = 0$ level and the $J = 2$ **e** and **f** Λ doublets of the $a\ ^1\Delta$ $v = 0$ level, equals 5.6 ± 1.5:1 with both scattering chamber pumps fully open (6×10^{-5} Torr chamber pressure and estimated residence time 35 ms). In obtaining this ratio, we took account of the degeneracy of the $a\ ^1\Delta$ level. We also investigated the dependence of this population ratio on the residence time in the scattering chamber in the same manner as described in Sec. III B. This ratio was measured with each diffusion pump valved off in turn. We obtained values of 6.8 ± 1.8 and 16.1 ± 4.3 for estimated residence times of 52 and 110 ms, respectively. If we assume that the quenching is a first-order decay process with respect to the number of wall and gas-phase collisions, and hence the residence time, we can extrapolate back to zero residence time. We find that the above population ratio extrapolates to 4.1 ± 1.2. These experimental results would appear to indicate that NH($a\ ^1\Delta$) is relatively inefficiently quenched upon collisions with the wall.

This population ratio can be converted into the ratio of $v = 0$ populations in the $X\ ^3\Sigma^-$ vs $a\ ^1\Delta$ states by noting that our derived rotational distributions indicate that 9% of the $X\ ^3\Sigma^-$ $v = 0$ level is in the $J = 4\ F_1$ fine-structure level and, correspondingly, 33% of the $a\ ^1\Delta$ $v = 0$ level is in $J = 2$. We thus find that the ratio of the populations in the $X\ ^3\Sigma^-$ $v = 0$ vs. $a\ ^1\Delta$ $v = 0$ manifolds is 15.1 ± 4.3:1, extrapolated to zero residence time. We present in Table II the inferred $X\ ^3\Sigma^-$ vibrational state populations relative to $a\ ^1\Delta$ $v = 0$. We can then derive an electronic state branching ratio if we sum over the populations in all vibrational levels in both electronic states. To take account of possible population in levels $v \geqslant 3$ of $a\ ^1\Delta$, we assume that they contribute a population equal to that for $v = 2$. We conclude that the NH product electronic state branching ratio equals 3.2 ± 1.3:1 for the $X\ ^3\Sigma^-$ vs. $a\ ^1\Delta$.

We were unable to detect NH product in the $b\ ^1\Sigma^+$ electronic state. The observed signal-to-noise ratio could be used to estimate an upper bound on the relative population in this state. We find that the ratio of the $b\ ^1\Sigma^+$ $v = 0$ to $a\ ^1\Delta$ $v = 0$ populations must be $\leqslant 0.02$. In deriving this number, we supposed that a temperature of 300 K would characterize the rotational distribution in the $b\ ^1\Sigma^+$ $v = 0$ manifold.

As has been discussed in detail previously,[44] this type of laser fluorescence experiment, strictly speaking, measures the densities n_f of molecules created in specific quantum states, while we desire to measure relative cross sections σ_f for formation, which are proportional to fluxes. Since the NH products appear to be rotationally equilibrated with the walls, we can assume that they are also translationally equilibrated and hence have the same laboratory velocity distribution. Hence, it is not necessary to perform the usual density-to-flux transformation. The populations reported in Table II can be taken to represent relative cross sections for formation of the various NH product vibronic levels. It should be pointed out that the excited $a\ ^1\Delta$ and $b\ ^1\Sigma^+$ states have very long radiative lifetimes[37,48–50] and are metastable with respect to the time scale of the experiment (residence time in the scattering chamber). Thus, radiative decay can be ignored as a loss process and the state ratios given in Table II should represent the nascent product distribution, provided we have properly corrected for collisional relaxation.

IV. DISCUSSION

The most interesting observation from this study of the dynamics of the H + N_3 reaction is the large $X\ ^3\Sigma^-$ to $a\ ^1\Delta$ electronic state branching ratio. While we have corrected the experimental ratio to zero residence time, there is obviously some uncertainty in this extrapolation. Nevertheless, it does appear that there is a significant yield of NH($X\ ^3\Sigma^-$) products in this reaction. Our conclusion that most of the NH reaction products are formed in the ground $X\ ^3\Sigma^-$ state rather than the $a\ ^1\Delta$ electronic state sharply contrasts with the behavior in the analogous F + N_3 reaction, in which it is thought that the bulk of the NF product is created in the $a\ ^1\Delta$ state.[9]

As outlined in the Introduction, there are two possible mechanisms for formation of NH in the $X\ ^3\Sigma^-$ state, namely spin–orbit mixing in the exit channel or direct reaction along the $^3A''$ surface. The former pathway is responsible for the production of ground state NH fragments in the IRMPD and NH overtone excited decomposition of HN_3.[27,28] The observed lifetimes[27(b)] for spin–forbidden dissociation to

NH($X\,^3\Sigma^-$) product provide indirect evidence for the probability of spin–orbit mixing in HN_3. These lifetimes are found to be at least 10^4 longer than predicted by a RRKM calculation in which the dissociation was treated as if it were spin-allowed. Yarkony[51] has calculated the spin–orbit matrix element between the HN_3 $\tilde{X}\,^1A'$ and $^3A''$ wave function for geometries near the crossing of these two surfaces in the exit channel. A simple Landau–Zener calculation based on these matrix elements suggests that the probability for singlet–triplet transitions will be very small (of the order of 1%) unless the velocity along the reaction coordinate (approximately the NH–N_2 separation) is very small. In the H + N_3 reaction, the total energy available to a HN_3 complex is significantly greater than in the NH overtone excitation experiments so that we would expect the dynamics in the bimolecular reaction to be even more diabatic. Thus, it is difficult to rationalize the observed relatively large NH $X\,^3\Sigma^-$ to $a\,^1\Delta$ state ratio in the H + N_3 reaction solely on the basis of spin–orbit mixing in the exit channel. This leads us to infer that formation of NH($X\,^3\Sigma^-$) products occurs through the $^3A''$ surface.

So far, our argument about the importance of the $^3A''$ surface as the path by which NH($^3\Sigma^-$) products are formed has centered on the large observed yield of ground state NH in comparison to that expected from the mechanism of singlet–triplet transitions from the $\tilde{X}\,^1A'$ surface in the exit channel. Let us now turn to a consideration of the $^3A''$ surface itself. Simple molecular orbital arguments can be used to justify the qualitative ordering of the energies of the various surfaces in Fig. 1 emanating from the H + N_3 asymptote. In the N_3 reagent, the π_g orbital, which can be described as the out-of-phase combination of $2p_{x,y}$ orbitals on the terminal nitrogen atoms, is singly occupied, while in the hydrogen atom the 1s orbital is singly occupied. The $\tilde{X}\,^1A'$ wave function, whose approximate electron configuration can be written[28,51,52] as $1a'^2...9a'^2 1a''^2 2a''^2$, arises from the in-phase combination of the H 1s orbital and the N_3 π_g component which lies in the H–N_3 plane. This surface will be strongly attractive because of the bonding nature of this interaction.

The $^3A''$ and $^1A''$ surfaces will arise from the interaction of the H 1s orbital and the out-of-phase N_3 π_g component and represent triplet and singlet spin coupling, respectively, of the unpaired electrons; the approximate electron configuration is given[28,51] by $1a'^2...9a'^2 10a' 1a''^2 2a''$. By Hund's rule we expect the former to be lower in energy, in a singlet-configuration description of the wave functions. The energetics of these surfaces relative to the reagents is uncertain. The first absorption band of HN_3 is located near 265 nm.[21,53] This most likely reflects the energy difference between the $\tilde{X}\,^1A'$ state and the first excited singlet, namely $^1A''$ state, at the ground state equilibrium geometry. This places the $^1A''$ state at approximately 78 kJ/mole above the H + N_3 asymptote. Hence, the $^1A''$ surface probably has too high a barrier to be involved in this reaction. Finally, the last surface emanating from the H + N_3 asymptote is $^3A'$ and is given by the out-of-phase combination of the H 1s orbital and the N_3 π_g component which lies in the H–N_3 plane. This surface is expected to be the highest in energy and is likely strongly repulsive.

The arguments given in the last two paragraphs allows us to deduce the relative ordering of the surfaces but will not reveal whether a possible barrier on the $^3A''$ surface is greater than the reagent translational energy (4 kJ/mole). Yarkony[51] has calculated the energy of the $^3A''$ surface at the experimental HN_3 ($\tilde{X}\,^1A'$) equilibrium geometry, as well as in the NH–N_2 exit channel. He finds that the $^3A''$ state lies 446 kJ/mole above the minimum on the $\tilde{X}\,^1A'$ surface. This energy must be corrected for the zero-point energies; for the $\tilde{X}\,^1A'$ state, this can be calculated from the experimental vibrational frequencies,[54] while for the $^3A''$ state this is approximated by the zero-point energy[55] of N_3 (assuming a H···N_3 structure). The $^3A''$ state is thus calculated to lie 414 kJ/mole above the ground vibrational level of HN_3($\tilde{X}\,^1A'$). This can be compared to the energy of the H + N_3 reactants (373 kJ/mole) relative to HN_3($\tilde{X}\,^1A'$); this value was obtained from the exothermicity given in Eq. (1) and the dissociation energy D(HN–N_2) = 45 ± 6 kJ/mole given by Okabe.[56] We thus see that the energy of the $^3A''$ state, at least at the equilibrium $\tilde{X}\,^1A'$ geometry, is comparable to that of the reactants. Moreover, no geometry search has been carried out so that it is not known whether this one point is on the minimum energy path for reaction. In fact, we expect from arguments[26] based on Walsh's rules that the NNN skeleton will be bent for the $^3A''$ surface. Further calculations on the energetics of the $^3A''$ surface in the entrance channel would help greatly in further understanding the reaction dynamics. Unfortunately, our rotational distributions of the NH products are relaxed so that the measured distributions of the Λ doublets or spin states cannot be used to answer the questions raised above.

In view of the fact that reaction appears to be occurring on both the $\tilde{X}\,^1A'$ and $^3A''$ HN_3 potential energy surfaces, it is interesting to see whether the NH $X\,^3\Sigma^-$ to $a\,^1\Delta$ state branching ratio can be explained simply by statistical arguments. Here we take the statistical formation rates as the prior distributions in a surprisal analysis.[57] Including the statistical weight of each electronic state (spin multiplicity times the Λ degeneracy),[58] we find that the statistical $X\,^3\Sigma^-$ to $a\,^1\Delta$ branching ratio is calculated to equal 10:1. Alternatively, the $X\,^3\Sigma^-$ to $a\,^1\Delta$ branching ratio may be expected to reflect the degeneracies of the two surfaces ($^3A''$ and $\tilde{X}\,^1A'$) on which these products are assumed to be formed, if the entrance barriers are negligible and there is no mixing. This model predicts a value of 3:1 for the electronic state branching ratio. Our experimentally observed state branching ratio of 3.2 ± 1.3:1 is close to the latter prediction.

The NH($a\,^1\Delta$) products from the H + N_3 reaction have been found to be formed with a significant degree of vibrational excitation. We estimate that the $a\,^1\Delta$ state is produced with an average vibrational excitation of 62 kJ/mole, or about 35% of the available energy in the NH($a\,^1\Delta$) + N_2 channel. It is interesting to compare these results with the vibrational distribution of NH($a\,^1\Delta$) formed in the UV photodissociation of HN_3. The reaction exothermicity of the H + N_3 reaction corresponds to a photolysis wavelength of 320 nm in the latter. No photodissociation experiments have been carried out at such a long wavelength; however, the

$v = 1$ to $v = 0$ ratio was found to equal 1:0.72 for photolysis at 248 nm.[23] It appears that the NH($a\ ^1\Delta$) products are formed with higher vibrational excitation in the H + N_3 reaction.

There have been two theoretical investigations of the dissociation of HN_3 to NH + N_2 products. Lievin *et al.*[52] observed that the NH and N_2 bond distances rapidly relaxed to the values appropriate to the isolated molecules as HN_3 dissociated on the $\tilde{X}\ ^1A'$ surface. This result was later confirmed by MCSCF-CI calculations with a larger basis set by Alexander *et al.*,[28] who also found that the diatomic fragment bond distances were already close to their asymptotic values at the lowest energy crossing point between the $\tilde{X}\ ^1A'$ and $^3A''$ surfaces. These results do not explain our observations of high vibrational excitation in NH($a\ ^1\Delta$). It may be that reaction along the singlet surface is better described as a direct abstraction reaction, rather than the decay of an activated complex: The estimated[27(b)] RRKM lifetime for $HN_3(\tilde{X}\ ^1A')$ with an energy content equal to that of the H + N_3 reagents is considerably less than 10^{-13} s. Thus, the H + N_3 reaction is similar to the well studied $O(^1D) + H_2$ reaction, in which the deep $H_2O(\tilde{X}\ ^1A')$ well is accessible but the OH products are formed with a nonstatistical state distribution.[59–61] The H + N_3 reaction is an example of a **L + HH** mass combination, whose product energy disposal is believed to be particularly sensitive to the degree of attractive energy release.[62] Indeed, in the H + O_3 reaction, the available energy is channeled almost exclusively into product OH vibration.[63]

In contrast with the NH($a\ ^1\Delta$) products, NH ($X\ ^3\Sigma^-$) is found to be formed with little vibrational excitation. This could simply be due to efficient vibrational relaxation of NH($X\ ^3\Sigma^-$) on the walls. However, it seems unlikely that the efficiency of vibrational relaxation of the $X\ ^3\Sigma^-$ and $a\ ^1\Delta$ states would be drastically different. The low vibrational excitation in NH ($X\ ^3\Sigma^-$) can alternatively be ascribed to the topology of the $^3A''$ surface. This surface is expected to be strongly repulsive, with the energy release occurring in the HN–NN exit channel. We would expect little vibrational excitation in the newly formed NH bond in this case.

From our derived NH internal state distributions, we conclude that the bulk of the reaction exoergicity appears in other product degrees of freedom, namely translational energy, N_2 internal excitation, and possibly NH rotational excitation. Unfortunately, the latter appears relaxed in this experiment. The N_2 internal state distribution could be determined by REMPI detection, as we have done for the N_2 fragment in the photodissociation of HN_3.[26] However, it is expected that there will be a considerable background of N_2, both from decomposition of N_3 in the prereactor and from photolysis of N_3 by the REMPI probe laser.

The H + N_3 reaction is sufficiently exothermic to allow production of NH in its $b\ ^1\Sigma^+$ state, as well as $X\ ^3\Sigma^-$ and $a\ ^1\Delta$. We find a negligible electronic state branching into NH($b\ ^1\Sigma^+$) in the H + N_3 reaction. This result can be rationalized with the qualitative potential energy surfaces shown in Fig. 1. The NH($b\ ^1\Sigma^+$) + N_2 asymptote correlates with the second $HN_3\ ^1A'$ surface, which arises from electronically excited H + N_3 reagents. Unless this $^1A'$ surface were strongly bound and hence were to cross the $^3A''$ or $\tilde{X}\ ^1A'$ surfaces, there will be no mechanism to allow formation of NH($b\ ^1\Sigma^+$) from H + N_3 with both reagents in their ground electronic states.

ACKNOWLEDGMENTS

We have benefitted from conversations with D. R. Yarkony, M. H. Alexander, S. Rosenwaks, F. Stuhl, D. S. King, and W. J. Marinelli about both theoretical and experimental topics connected with the study of this reaction. We are also grateful to H. H. Nelson and J. R. McDonald for providing us with unpublished NH band radiative transition probabilities. This work has been supported by the Air Force Office of Scientific Research under Contract No. F49620-88-C-0056 and by the National Science Foundation under Grant No. CHE-8700970. Travel support from the U. S. Israel Binational Science Foundation is also gratefully acknowledged.

APPENDIX: THE USE OF LASER FLUORESCENCE DETECTION TO MEASURE ELECTRONIC STATE BRANCHING RATIOS

Greene and Zare[40] have derived the basic equation relating fluorescence intensities to rotational populations within a given vibrational level. The fluorescence intensity in the $J' \rightarrow J''$ emission line for a transition from the level J to be detected (whose population, summed over the M_J levels, equals n_J) to excited level J' is given by

$$I(J,J',J'';\hat{\varepsilon}_a,\hat{\varepsilon}_d) = C\,[n_J/(2J+1)]S_{J'J}S_{J'J''}R_{JJ'J''}, \tag{A1}$$

where C includes the laser pulse energy, detection geometry factors, etc. The factors $S_{J'J}$ and $S_{J'J''}$ are the rotational line strength factors for the absorption and emission processes, respectively. The factor $R_{JJ'J''}$ depends on the laser and detector polarization directions $\hat{\varepsilon}_a$ and $\hat{\varepsilon}_d$ respectively, and, for an isotropic M_J distribution, equals

$$R_{JJ'J''} = \left[\frac{1}{9(2J'+1)} + \frac{2}{3}(-1)^{J-J''}\begin{Bmatrix} J' & J' & 2 \\ 1 & 1 & J \end{Bmatrix} \times \begin{Bmatrix} J' & J' & 2 \\ 1 & 1 & J'' \end{Bmatrix} P_2(\cos\chi_{ad})\right], \tag{A2}$$

where χ_{ad} is the angle between $\hat{\varepsilon}_a$ and $\hat{\varepsilon}_d$. In usual experiments, the fluorescence wavelength and polarization are not resolved so that sums over J'' and $\hat{\varepsilon}_d$ are taken in Eq. (A1).[44]

The application of Eq. (A1) to comparing populations in different electronic states, e.g., the $X\ ^3\Sigma^-$ and $a\ ^1\Delta$ states of NH, has not been considered explicitly previously and may have some ambiguities because of the possible different normalizations of rotational line strength factors and electronic transition moments.[42,64] We modify Eq. (A1) by including explicitly the vibronic and fine-structure labels for the upper and lower states in the excitation transition and including the sum over the final states and $\hat{\varepsilon}_d$. We also need to include explicitly the detection sensitivity since different electronic transitions will be observed in fluorescence. Equa-

tion (A1) now reads

$$I(iv'J'p';jvJp;\hat{\varepsilon}_a) = C[n_{jvJp}/(2J+1)]S_{iv'J'p';jvJp} \times \sum_{\hat{\varepsilon}_d} \sum_{v''J''p''} \mathscr{S}_{iv'J'p';jv''J''p''} R_{JJ'J''}, \quad \text{(A3)}$$

where $S_{iv'J'p';jvJp}$ is the line strength factor for the $iv'J'p' \leftarrow jvJp$ transition and $\mathscr{S}'_{iv'J'p';jv''J''p''}$ is the sensitivity of detection of emission on the $iv'J'p' \rightarrow jv'J''p''$ transition. The latter is given by the probability P that the excited state emits on this transition times the detected photomultiplier signal:

$$\mathscr{S}_{iv'J'p';jv''J''p''} = h\nu_{iv';jv''} D(\lambda_{iv';jv''})P, \quad \text{(A4)}$$

where $D(\lambda_{iv';jv''})$ is the energy sensitivity at this wavelength. The factor P in Eq. (A4) equals

$$P = \tau_{v'} A_{iv'J'p';jv''J''p''}, \quad \text{(A5)}$$

where $\tau_{v'}$ is the excited state radiative lifetime and the spontaneous transition probability is given by[42,64]

$$A_{iv'J'p';jv''J''p''} = (64\pi^4/3h)\nu^3_{iv';jv''} S_{iv'J'p';jv''J''p''} (2J'+1)^{-1}. \quad \text{(A6)}$$

We have assumed that the wavelength varies negligibly in a vibrational band.

As is usually done,[42] we factor the line strength factors $S_{iv'J'p';jv''J''p''}$ in Eqs. (A3) and (A6) into a vibronic and rotational term:

$$S_{iv'J'p';jv''J''p''} = S_{iv';jv''} S_{J'p';J''p''}. \quad \text{(A7)}$$

We follow the convention proposed by Whiting *et al.*[42] so that the sum rule for the rotational line strengths $S_{J'p';J''p''}$ follows their Eq. (4). It should be noted that our factor $S_{iv';jv''}$ represents $q_{v'v''}|R_e|^2$ in their Eq. (3). Substituting Eqs. (A4) through (A7) into Eq. (A3), we obtain the fluorescence intensity as

$$I(iv'J'p';jvJp;\hat{\varepsilon}_a) = C[n_{jvJp}/(2J+1)]S_{iv';jv}S_{J'p';Jp}\mathscr{S}_{iv'} \times \sum_{\hat{\varepsilon}_d} \sum_{J''p''} S_{J'p';J''p''} R_{JJ'J''} \times [(2-\delta_{0,\Lambda'})/(2-\delta_{0,\Lambda'+\Lambda''})]. \quad \text{(A8)}$$

The factor $(2J'+1)^{-1}$ in Eq. (A6) was not included in Eq. (A8) since this factor is already taken into account in $R_{JJ'J''}$ [Eq. (A2)]. The term in square brackets in Eq. (A8) equals 1/2 for a $\Sigma \leftarrow \Pi$ transition and 1 otherwise and arises from the rotational sum, discussed below.

The sensitivity $\mathscr{S}_{iv'}$ of detection of the excited vibrational level v' is given by

$$\mathscr{S}_{iv'} = \tau_{v'} \sum_{v''} h\nu_{iv';jv''} D(\lambda_{iv';jv''}) A_{iv';jv''}. \quad \text{(A9)}$$

The vibronic line strength factors $S_{iv';jv''}$ are often obtained from band transition probabilities $A_{iv';jv''}$. Larsson[64] has shown that, with the convention of Whiting *et al.*[42] for the electronic transition moment, these quantities are related in the following way:

$$A_{iv';jv''} = (64\pi^4/3h)\nu^3_{iv';jv''} S_{iv';jv''} \times [(2-\delta_{0,\Lambda'+\Lambda''})/(2-\delta_{0,\Lambda'})]. \quad \text{(A10)}$$

The term in square brackets in Eqs. (A8) and (A10) appear since the sum of the rotational line strengths $S_{J'p';J''p''}$ over the lower state labels $J''p''$ equals $(2J'+1)$ for all transitions except $\Pi \rightarrow \Sigma$, for which the sum equals $2(2J'+1)$.

Equation (A8) is our working equation for the comparison of populations in different electronic states, as detected by laser fluorescence excitation. The factors $S_{iv';jv''}$ and $\mathscr{S}'_{iv'}$ were calculated using the radiative lifetimes reported by Stuhl and coworkers[39,47] and the band emission probabilities $A_{iv';jv''}$ reported by Nelson and McDonald on the c–a system[25] and those calculated by Yarkony[37] for the A–X system. The detector sensitivity $D(\lambda_{iv';jv''})$ is given by the product of the sensitivity of the photomultiplier (obtained from the manufacturer's specifications) and the transmission of the bandpass filter. In all cases, only one vibronic band was observed in emission.

[1] See, for example, F. Kaufman, J. Phys. Chem. **88**, 4909 (1984); M. J. Howard and I. W. M. Smith, Prog. React. Kinet. **12**, 55 (1983).
[2] For reviews of work on this reaction, see D. Klenerman and I. W. M. Smith, J. Chem. Soc. Faraday Trans. 2 **83**, 229 (1987); S. J. Wategaonkar and D. W. Setser, J. Chem. Phys. **90**, 251 (1989).
[3] D. G. Sauder and P. J. Dagdigian, J. Chem. Phys. **92**, 2389 (1990); A. M. L. Irvine, I. W. M. Smith, and R. P. Tuckett, *ibid.* (submitted).
[4] S. J. Wategaonkar and D. W. Setser, J. Chem. Phys. **90**, 6223 (1989).
[5] R. J. Malins and D. W. Setser, J. Phys. Chem. **85**, 1342 (1981); C. T. Cheah and M. A. A. Clyne, J. Chem. Soc. Faraday Trans. 2 **76**, 1543 (1980).
[6] T. C. Clark and M. A. A. Clyne, Trans. Faraday Soc. **66**, 877 (1970).
[7] R. D. Coombe and A. T. Pritt, Jr., Chem. Phys. Lett. **58**, 606 (1978); A. T. Pritt, Jr., and R. D. Coombe, Int. J. Chem. Kinet. **12**, 741 (1980).
[8] A. T. Pritt, Jr., D. Patel, and R. D. Coombe, Int. J. Chem. Kinet. **16**, 977 (1984).
[9] J. Habdas, S. Wategaonkar, and D. W. Setser, J.Phys. Chem. **91**, 451 (1987).
[10] L. G. Piper, R. H. Krech, and R. L. Taylor, J. Chem. Phys. **71**, 2099 (1979).
[11] K. Yamasaki, T. Fueno, and O. Kajimoto, Chem. Phys. Lett. **94**, 425 (1983).
[12] (a) S. J. David and R. D. Coombe, J. Phys.Chem. **89**, 5206 (1985); (b) S. J. David and R. D. Coombe, *ibid.* **90**, 3260 (1986).
[13] W. J. Marinelli (private communication).
[14] T. L. Henshaw, M. A. MacDonald, D. H. Stedman, and R. D. Coombe, J. Phys. Chem. **91**, 2838 (1987).
[15] T. L. Henshaw, D. McElwee, D. H. Stedman, and R. D. Coombe, J. Phys. Chem. **92**, 4606 (1988).
[16] D. J. May and R. D. Coombe, J. Phys. Chem. (in press).
[17] The enthalpy change for Eq. (1) was obtained by using $\Delta H^0_f(N_3) = 468.6 \pm 20.9$ kJ mole^{-1} [M. J. Pellerite, R. L. Jackson, and J. I. Brauman, J. Phys. Chem. **85**, 1624 (1981); E. Illenberger, P. B. Comita, J. I.Brauman, H.-P. Fenzlaff, M. Heni, N. Heinrich, W. Koch, and G. Frenking, Ber. Bunsenges. Phys. Chem. **89**, 1026 (1985)] and $\Delta H^0_f(NH) = 357 \pm 1$ kJ mole^{-1} [W. R. Anderson, J. Phys.Chem. **93**, 530 (1989)].
[18] J. Chen, E. Quiñones, and P.J. Dagdigian, J. Chem. Phys. **90**, 7603 (1989).
[19] A. C. Becker, J. Langen, M. H. Oberhoffer, and U. Schurath, J. Chem. Phys. **84**, 2907 (1986); R. D. Coombe and M. H. Van Benthem, *ibid.* **81**, 2984 (1984); D. R. Yarkony, *ibid.* **86**, 1642 (1987); and references therein.
[20] R. F. Heidner III, H. Helvajian, J. S. Holloway, and J. B. Koffend, J. Phys. Chem. **93**, 7813 (1989).
[21] A. P. Baronavski, R. G. Miller, and J. R. McDonald, Chem. Phys. **30**, 119 (1978).
[22] L. G. Piper, R. H. Krech, and R. L. Taylor, J. Chem. Phys. **73**, 791 (1980).
[23] F. Rohrer and F. Stuhl, J. Chem. Phys. **88**, 4788 (1988).
[24] K.-H. Gericke, R. Theinl, and F. J. Comes, J. Chem. Phys, **92**, 6548 (1990).
[25] H. H. Nelson and J. R. McDonald, J. Chem. Phys. (submitted).

[26] J.-J. Chu, P. Marcus, and P. J. Dagdigian, J. Chem. Phys. **93**, 257 (1990).
[27] (a) J. C. Stephenson, M. P. Casassa, and D. S. King, J. Chem. Phys. **89**, 1378 (1988); (b) B. R. Foy, M. P. Casassa, J. C. Stephenson, and D. S. King. *ibid.* **89**, 608 (1988); **90**, 7037 (1989); **92**, 2782 (1990).
[28] M. H. Alexander, H.-J. Werner, and P. J. Dagdigian, J. Chem. Phys. **89**, 1388 (1988).
[29] E. J. Murphy and J. H. Brophy, Rev. Sci. Instrum. **50**, 635 (1979).
[30] M. A. A. Clyne, in *Reactive Intermediates in the Gas Phase*, edited by D. W. Setser (Academic, New York, 1979), p. 2.
[31] B. Krakow, R. C. Lord, and G. O. Neely, J. Mol. Spectrosc. **27**, 148 (1968).
[32] C. R. Brazier, R. S. Ram, and P. F. Bernath, J. Mol. Spectrosc. **120**, 381 (1986).
[33] R. S. Ram and P.F. Bernath, J. Opt. Soc. Am. B **3**, 1170 (1986).
[34] R. W. Lunt, R. W. B. Pearse, and E. C. W. Smith, Proc. R. Soc. London Ser. A **15**, 173 (1936).
[35] F. L. Whittaker, J. Phys. B **1**, 977 (1968).
[36] J. M. Lents, J. Quant. Spectrosc. Radiat. Transfer **13**, 297 (1973).
[37] D. R. Yarkony, J. Chem. Phys. **91**, 4745 (1989).
[38] W. H. Smith, J. Brzozowski, and P. Erman, J. Chem. Phys. **64**, 4628 (1976).
[39] R. D. Kenner, F. Rohrer, and F. Stuhl, J. Phys. Chem. **93**, 7824 (1989).
[40] C. H. Greene and R. N. Zare, J. Chem. Phys. **78**, 6741 (1983).
[41] R. N. Zare, in *Molecular Spectroscopy; Modern Research*, edited by K. N. Rao and C. W. Mathews (Academic, New York, 1972), p.207.
[42] E. E. Whiting, A. Schadee, J. B. Tatum, J. T. Hougen, and R. W. Nicholls, J. Mol. Spectrosc. **80**, 249 (1980).
[43] P. J. Dagdigian, J. Chem. Phys. **90**, 6110 (1989).
[44] P. J. Dagdigian, in *Atomic and Molecular Beam Methods*, Vol. 1, edited by G. Scoles, D. Bassi, U. Buck, and D. Lainé (Oxford University, New York, 1988), Chap. 23.
[45] See, for example, M. L.Campbell and P. J. Dagdigian, Faraday Discuss. Chem. Soc. **84**, 127 (1987).
[46] F. Stuhl (private communication).
[47] R. D. Kenner, A. Kaes, R. K. Browarzik, and F. Stuhl, J. Chem. Phys. **91**, 1440 (1989).
[48] C. M. Marian and R. Klotz, Chem. Phys. **95**, 213 (1985).
[49] U. Blumenstein, F. Rohrer, and F. Stuhl, Chem. Phys. Lett. **107**, 347 (1984).
[50] A. Ramsthaler-Sommer, K. E. Eberhardt, and U. Schurath, J. Chem. Phys. **85**, 3760 (1984).
[51] D. R. Yarkony, J. Chem. Phys. **92**, 320 (1990).
[52] J. Lievin, J. Breulet, and G. Verhaegen, Theoret. Chim. Acta **52**, 75 (1979).
[53] J. W. Rabalais, J. R. McDonald, V. Scherr, and S. P. McGlynn, Chem. Rev. **71**, 73 (1971).
[54] T. Shimanouchi, J. Phys. Chem. Ref. Data **6**, 993 (1977).
[55] M. E. Jacox, J. Phys. Chem. Ref. Data **17**, 269 (1988); C. R. Brazier, P. F. Bernath, J. B. Burkholder, and C. J. Howard, J.Chem. Phys. **89**, 1762 (1988); R. Tian, J. C. Facelli, and J. Michl, J. Phys. Chem. **92**, 4073 (1988).
[56] H. Okabe, *Photochemistry of Small Molecules* (Wiley, New York, 1978).
[57] R. B. Bernstein and R. D. Levine, Adv. At. Mol. Phys. **11**, 215 (1975).
[58] M. H. Alexander and P.J. Dagdigian, Chem. Phys. **33**, 13 (1978).
[59] A. C. Luntz, R. Schinke, W. A. Lester, Jr., and Hs. H. Gunthard, J. Chem. Phys. **70**, 5908 (1979); A. C. Luntz, *ibid.* **73**, 1143 (1980).
[60] G. K. Smith and J. E. Butler, J. Chem. Phys. **73**, 2243 (1980).
[61] J. E. Butler, G. M. Jursich, I. A. Watson, and J. R. Wiesenfeld, J. Chem. Phys. **84**, 5365 (1986); C. B. Cleveland, G. M. Jursich, M.Trolier, and J. R. Wiesenfeld, *ibid.* **86**, 3253 (1987).
[62] P. J. Kuntz, E. M. Nemeth, J. C. Polanyi, S. D. Rosner, and C. E. Young, J. Chem. Phys. **44**, 1168 (1966).
[63] J. C. Polanyi and J. J. Sloan, Int. J. Chem. Kinet. Symp. **1**, 51 (1975).
[64] M. Larsson, Astron. Astrophys. **128**, 291 (1983).